Cascaded Estimation Architecture for Integration of Foot-Mounted Inertial Sensors

Bernhard Krach and Patrick Roberston
German Aerospace Center (DLR)

***Abstract*— An algorithm for integrating foot-mounted inertial sensor platforms is presented. The proposed integration scheme is based on a cascaded estimation architecture. A lower Kalman filter is used to estimate the step-wise change of position and direction of one or optionally both feet respectively. These estimates are used in turn as measurements in an upper particle filter, which is able to incorporate nonlinear map-matching techniques. To ease the integration of both feet a simple mechanical pedestrian model is developed. The proposed algorithm is verified using computer simulations and experimental data.**

***Index Terms*— Pedestrian Navigation, Inertial Integration, Indoor Navigation, Map-Matching**

I. Introduction

The use of inertial sensors is becoming widespread for pedestrian navigation, especially for indoor applications. Basically two approaches can be distinguished. The pedometer-approach employs an accelerometer for detecting individual steps whilst the stride length and stride direction are themselves estimated using additional sensors, such as global navigation satellite systems (GNSS), or a priori information. Given a detected step, its length and its direction, a person's position can be determined by dead-reckoning [1], [2], [3]. Other methods have been studied in [4]. The latest approaches are based on full six degree of freedom (6DOF) inertial navigation. A foot-mounted 6DOF strapdown inertial platform comprising triads of accelerometers and gyroscopes is used to dead reckon via a conventional strapdown navigation algorithm. An indirect feedback extended Kalman filter runs in parallel to the strapdown algorithm. Rest phases of the foot, which are detected from the accelerometer signals, trigger zero-velocity (virtual) measurements that are used to update the filter (ZUPT). Due to the regular ZUPT measurements we can estimate and correct the drift errors, which accumulate in the strapdown solution [5], [6], [7], [8]. It was shown in [5] that this approach can achieve very good performance even with today's low-cost micro-electro-mechanical (MEMS) sensors, because the ZUPTs are so frequent that errors build up only slowly during each step the pedestrian makes. Nevertheless the proposed Kalman filter approach is not optimal, as the algorithm does not take into account prior dynamic knowledge about the motion of the pedestrian or the motion of her foot and there is no mathematically sound procedure when considering the incorporation of nonlinear map-matching techniques or additional nonlinear / non-Gaussian sensors typically used in an indoor scenario.

To address this here we propose a cascaded estimation architecture: To estimate the foot's navigation parameters we use a state-of-the-art integration filter comprising a conventional strapdown navigation algorithm along with an indirect feedback extended Kalman filter and a ZUPT detection algorithm for the foot that is suitably equipped with a 6DOF inertial sensor suite [5]. For each step we compute foot displacement and heading change values from the foot's filter and exploit them as measurements within a higher-level main fusion (particle) filter, which is able to consider the nonlinear dynamics of the human by means of a dedicated pedestrian movement model, including also maps and building constraints. This approach, which operates at a much lower sampling rate, has been shown to be highly valuable, in particular in an indoor scenario [9], [10]. Based on a simple mechanical pedestrian model interconnecting the pedestrian's body and his feet it is shown that the same approach is still viable when integrating a pair of platforms that are mounted on each of the pedestrians' feet respectively. It is shown that in this case the accuracy of the dead-reckoning is doubled.

The paper is organized as follows: At first a brief review of sequential Bayesian estimation and particle filtering is given. Subsequently our integration approach is motivated and details on the filter design are addressed, including the extension towards a pair of platforms. Computer simulation results and experimental results conclude the paper.

II. Sequential Estimation

A. Optimal Solution

The task of a navigation system is commonly to estimate successively a set of navigation parameters, here referred to as the hidden state $\mathbf{x}_k$, based on an evolving sequence of noisy measurements $\mathbf{z}_k$ (over the temporal index k). If the future state given the present state and all its past states depend only on the present state (and not on any past states), the temporal evolution of navigation parameters can be modeled as a first-order Markov process . If it is also assumed that the noise affecting successive measurements is independent of the past noise values, such that each observation depends only on the present state, the optimal solution is given by the application of *sequential Bayesian estimation*. The reader is referred to [11] which gives a derivation of the general framework for optimal estimation of temporally evolving (Markovian) parameters by means of inference; and we have chosen similar notation. The entire history of observations can be written as

$$\mathbf{Z}_k \widehat{=} \{\mathbf{z}_q, q = 1, \ldots, k\} \ , \tag{1}$$

It can be shown that the sequential estimation algorithm is

recursive, as it uses the posterior PDF computed for time instance $k-1$ to compute the posterior PDF for instance k . For a given posterior PDF at time instance $k-1$, $p(\mathbf{x}_{k-1}|\mathbf{Z}_{k-1})$, the *prior* PDF $p(\mathbf{x}_k|\mathbf{Z}_{k-1})$ is calculated in the so-called *prediction step* by applying the Chapman-Kolmogorov equation:

$$p(\mathbf{x}_k|\mathbf{Z}_{k-1}) = \int p(\mathbf{x}_k|\mathbf{x}_{k-1})p(\mathbf{x}_{k-1}|\mathbf{Z}_{k-1})\mathrm{d}\mathbf{x}_{k-1} \ , \quad (2)$$

with $p(\mathbf{x}_k|\mathbf{x}_{k-1})$ being the state transition PDF of the Markov process. In the *update step* the new posterior PDF for step k is obtained by applying Bayes' rule to $p(\mathbf{x}_k|\mathbf{z}_k, \mathbf{Z}_{k-1})$ yielding the normalized product of the likelihood $p(\mathbf{z}_k|\mathbf{x}_k)$ and the prior PDF:

$$\begin{aligned} p(\mathbf{x}_k|\mathbf{Z}_k) &= p(\mathbf{x}_k|\mathbf{z}_k, \mathbf{Z}_{k-1}) \\ &= \frac{p(\mathbf{z}_k|\mathbf{x}_k, \mathbf{Z}_{k-1})p(\mathbf{x}_k|\mathbf{Z}_{k-1})}{p(\mathbf{z}_k|\mathbf{Z}_{k-1})} \\ &= \frac{p(\mathbf{z}_k|\mathbf{x}_k)p(\mathbf{x}_k|\mathbf{Z}_{k-1})}{p(\mathbf{z}_k|\mathbf{Z}_{k-1})} \ . \end{aligned} \quad (3)$$

B. Suboptimal Solutions

The optimal estimation algorithm relies on evaluating the integral (2), which is usually a very difficult task, except for certain additional restrictions imposed on the model and the noise process. Thus beside the restricted optimal algorithms such as the Kalman filter or the grid-based methods, a large number of suboptimal algorithms exist, e.g. the extended and the Sigma-Point Kalman Filter, which are nonlinear adaptations of the generic Kalman filter concept [12].

A further family of suboptimal algorithms are the Sequential Monte Carlo (SMC) filters [11], [13]. In these algorithms the posterior density at step k is represented as a sum, and is specified by a set of N_p particles:

$$p(\mathbf{x}_k|\mathbf{Z}_k) \approx \sum_{j=1}^{N_p} w_k^j \cdot \delta(\mathbf{x}_k - \mathbf{x}_k^j) \ , \quad (4)$$

where each particle with index j has a state $\mathbf{x}_k^j$ and has a *weight* w_k^j. The sum over all particles' weights is one. The SMC filters are not restricted with respect to the model and the noise process, but the number of particles is a crucial parameter, as only for $N_p \rightarrow \infty$ does the approximate posterior approach the true PDF. The particles are drawn according to a so-called proposal density, $q(\mathbf{x}_k|\mathbf{x}_k^j, \mathbf{z}_k)$, such that their respective weight is calculated using

$$w_k^j \propto w_{k-1}^j \frac{p(\mathbf{z}_k|\mathbf{x}_k^j)p(\mathbf{x}_k^j|\mathbf{x}_{k-1}^j)}{q(\mathbf{x}_k^j|\mathbf{x}_{k-1}^j, \mathbf{z}_k)} \ . \quad (5)$$

Details on the proposal density used here can be found in [9].

C. Incorporation of Independent Sensors

This section deals with the case where a range of M sensor outputs makes up the overall measurement vector $\mathbf{z}_k$. Separating the measurement vector $\mathbf{z}_k$ into sub-vectors for each sensor

$$\mathbf{z}_k \widehat{=} \{\mathbf{z}_{m,k}, m = 1, \ldots, M\} \ , \quad (6)$$

and writing $\mathbf{z}_{m,k}^-$ for $\mathbf{z}_k$ after omitting $\mathbf{z}_{m,k}$, i.e. $\mathbf{z}_{m,k}^- = \mathbf{z}_k \backslash \mathbf{z}_{m,k}$. If we assume independent perturbations of the sub-vectors then this is equivalent to writing

$$p(\mathbf{z}_{m,k}|\mathbf{x}_k, \mathbf{z}_{m,k}^-) = p(\mathbf{z}_{m,k}|\mathbf{x}_k) \ , \quad (7)$$

so that given the actual state, the measurements $\mathbf{z}_{m,k}^-$ will not affect the measurement $\mathbf{z}_{m,k}$. In this case the overall likelihood function can be written in product form according to the factorization of Bayes' rule [14] as

$$p(\mathbf{z}_k|\mathbf{x}_k) = C \cdot \prod_{m=1}^{M} p(\mathbf{z}_{m,k}|\mathbf{x}_k) \quad (8)$$

with C being a normalizing constant. In other words, the sensors can be incorporated into the weight update (5) by simple multiplication.

III. Integration of Inertial Sensors

A. Motivation of Cascaded Approach

The most widespread approach to integrate strapdown inertial sensors into a navigation system is to use a direct/indirect extended Kalman filter together with a strapdown navigation computer [15], [16], [17]. The combination of the two algorithms may be interpreted as a "probabilistic" inertial navigation system (INS) and allows to calculate an approximation of the posterior PDF of position, velocity, attitude, and sensor errors based on the sequence of measurement received from the sensors of the 6DOF inertial platform. The approximated posterior/prior PDF is a Gaussian, whose mean is given by the strapdown solution corrected by the Kalman filter state vector and whose covariance matrix is given by the covariance matrix of the Kalman filter. The advantage of this approach is that the resulting Gaussian PDF can be joined analytically with linear/linearized Gaussian likelihoods of further sensors during the filter update step (5) as described in the previous section.

Despite the fact that the Kalman filter implements a Bayesian filter, this integration approach suffers from the major drawback that it does not follow (2) and (3) straightforwardly for two reasons:

- The Kalman filter indeed uses a probabilistic state transition model, but this model is based solely on pure kinematic relations between velocity, position, attitude, and sensor errors rather than on a true probabilistic characterization of the dynamics of the tracked object (e.g. a person traveling by foot).
- No likelihood function is used to incorporate the accelerometer and gyroscope measurements into the algorithm. Accelerometer and gyroscope measurements enter the algorithm directly via the strapdown computations and no explicit use is made of any prior knowledge about the object's dynamics. As a consequence the performance of a conventional INS is mainly determined by the quality of the inertial sensors.

To overcome this drawback it would indeed be optimal to formulate a Bayesian estimator whose dynamic model characterizes - besides position, velocity, attitude, and sensor

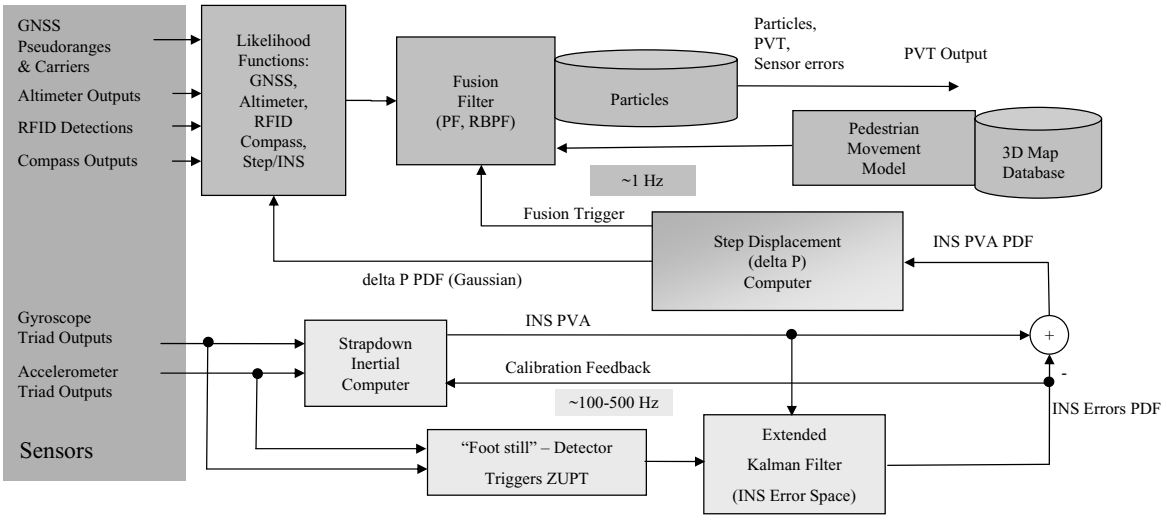

Fig. 1. Cascaded estimation architecture with upper particle filter (dark gray) including the fusion with further sensors and lower Kalman filter for stride estimation (light gray)

errors - also accelerations and turn rates of the navigating object using a Markov chain whose state transitions occur at the sensor measurement rate, which is relatively high for inertial sensors. Due to nonlinear state evolution constraints this can be generally a very difficult task, especially when considering a Markov-chain characterization of a pedestrian and the motion of her foot. Because of this, currently only the conventional integration approach seems to be feasible in order to estimate just the foot's movement for each step. Indeed, for the considered application of foot-mounted inertial sensors this is not a major drawback, as the inertial sensor errors can be constrained efficiently through the use of ZUPT measurements.

However, it is generally desirable to consider further prior dynamic knowledge about the pedestrian in an overall navigation filter. To take benefit of both the accurate foot-mounted inertial system and a dedicated pedestrian movement model including nonlinear effects such as building plans we propose a cascaded estimation architecture as illustrated in Figure 1. We have decided to employ a particle filter framework for the upper level fusion filter. This is because we will include sensors and process models (movement models) that are nonlinear, and often with non-Gaussian noise models. In particular the movement model needs to incorporate the building plan which is highly nonlinear. A lower Kalman filter is used to provide stepwise computed values of foot displacement and heading change, here referred to as the step-measurement, which is used as measurements within the upper particle filter and enters the algorithm via a Gaussian likelihood function along with the measurements and likelihoods of further available sensors.

Our framework has been implemented in Java and can process incoming sensor data in real-time, allowing live visualization of the location estimate. The filter will perform sensor fusion roughly every second or when triggered to do so by a specific sensor - in our case we will perform an update cycle at the latest once every second and also upon each step-measurement.

To distinguish the low rate operations of the upper filter from the high rate operations of the lower filter below, the terms k-*rate* and l-*rate* are introduced. The upper filter is associated to the k-rate, which is approximately the step-rate, and the lower filter is associated to the l-rate, which is given by the rate of the inertial sensors. Corresponding variables will be indicated by the subscripts $(\bullet)_k$ and $(\bullet)_l$.

B. Upper Filter

The particle filter adopts re-sampling of the particles at every time step. With exception of the step-measurement it adopts the state transition probabilities as proposal function and uses the product of the sensors' likelihood functions in the weight computation (8), (5) - the standard SIR formulation [11]. The incorporation of the INS-step-measurement, however, does not follow this approach [9]

1) State Model: In the particle filter we keep track of the pedestrians position $\mathbf{r}_k$ and her heading Ψ_k. To allow the incorporation of the step-measurement the state vector has been extended by the step-states $\Delta\mathbf{r}_k$ and $\Delta\Psi_k$, which relate $\mathbf{r}_k$ and Ψ_k to the time index $k-1$ (see III-B.3).

$$\mathbf{x}_k = \begin{pmatrix} \mathbf{r}_k \\ \Psi_k \\ \Delta\mathbf{r}_k \\ \Delta\Psi_k \end{pmatrix} \tag{9}$$

2) Measurement Model: The step-measurement $\mathbf{z}_k$, which will be the only used measurement within the scope of this paper, is assumed to depend only on the current state $\mathbf{x}_k$ and a noise term $\mathbf{n}_\Delta$:

$$\mathbf{z}_k = h(\mathbf{x}_k, \mathbf{n}_\Delta) \ . \tag{10}$$

In particular we use

$$\mathbf{z}_k = \begin{pmatrix} \Delta\mathbf{r}_k \\ \Delta\Psi_k \end{pmatrix} + \mathbf{n}_\Delta \ , \tag{11}$$

with $\mathbf{n}_\Delta$ being zero-mean element-wise uncorrelated Gaussian noise. The variances are adjusted to reflect the uncertainty of the step-measurement.

3) Movement Model: A probabilistic movement model is used to characterize the temporal evolution of a state $\mathbf{x}_k$. Given that this evolution follows a Markov process the movement can be characterized by a transitional density $p(\mathbf{x}_k|\mathbf{x}_{k-1})$, and our model follows the Markovian approach. The movement model used here aims to reflect the physical constraints that are imposed on the movement of a pedestrian, in particular in an indoor scenario, where walls can have a large impact. Formally, the new state $\mathbf{x}_k$ is assumed to depend only on the previous state $\mathbf{x}_{k-1}$ and a noise term $\mathbf{n}_d$:

$$\mathbf{x}_k = f(\mathbf{x}_{k-1}, \mathbf{n}_d) \ . \tag{12}$$

Here we have chosen that the new location and heading depend deterministically on the past state (and on the current state through the Δ-states):

$$\mathbf{r}_k = \mathbf{r}_{k-1} + \mathbf{C}(\Psi_{k-1})\Delta\mathbf{r}_k \ , \tag{13}$$

$$\Psi_k = \Psi_{k-1} + \Delta\Psi_k \ , \tag{14}$$

$\mathbf{C}(\Psi_{k-1})$ is the rotation matrix:

$$\mathbf{C}(\bullet) = \begin{pmatrix} \cos(\bullet) & -\sin(\bullet) & 0 \\ \sin(\bullet) & \cos(\bullet) & 0 \\ 0 & 0 & 1 \end{pmatrix} \ . \tag{15}$$

However, the probabilistic part of the movement movement model is incorporated into the temporal evolution of the displacement states $\Delta\mathbf{r}_k$ and $\Delta\Psi_k$:

$$\Delta\mathbf{r}_k = f(\mathbf{x}_{k-1}, \mathbf{n}_r) \ , \tag{16}$$

$$\Delta\Psi_k = g(\mathbf{x}_{k-1}, \mathbf{n}_\Psi) \ , \tag{17}$$

which depend only on the past state $\mathbf{x}_{k-1}$ and the noise terms $\mathbf{n}_r$ and $\mathbf{n}_\Psi$. The nonlinearity that is imposed by the walls is included in (16) in that the displacement of the location $\Delta\mathbf{r}_k$ depends on the presence of nearby walls and obstacles.

A very simple movement model is used here: Given that a displacement $\Delta\mathbf{r}_k$ intersects with one of the walls that are stored in the map database, we assign it the probability $p(\mathbf{x}_k|\mathbf{x}_{k-1}) = 0$. In other situations, if a wall has not been crossed, we want to draw according to:

$$\Delta\mathbf{r}_k = \mathbf{n}_r \ , \tag{18}$$

$$\Delta\Psi_k = n_\Psi \ , \tag{19}$$

where $\mathbf{n}_r$ and n_Ψ are drawn from mutually uncorrelated zero-mean white Gaussian noise processes, whose variances are adapted to the movement of a pedestrian. Despite the fact that this model is suitable for the case of a wall crossing, it is quite coarse otherwise, as is does not adequately represent the probability with which a pedestrian will move, given a known building layout or map [18]. To alleviate this, future work will incorporate more accurate movement models than the one used here.

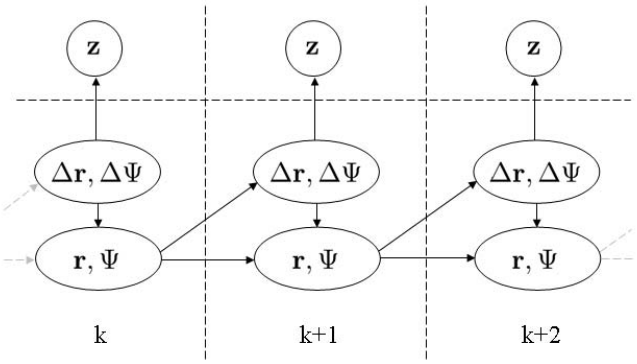

Fig. 2. Dynamic Bayesian network illustration of the pedestrian model used in the upper particle filter

An illustration of the pedestrian model used here in terms of a dynamic Bayesian network is shown in Figure 2.

C. Lower Filter

As the integration method proposed in [5] was shown to have both good performance and low complexity, we also follow this approach for the step estimation algorithm. The lower filter operates at the rate given by the output of the 6DOF sensor suite, which is in the range of 100–500 Hz, depending on the hardware settings.

1) Algorithm Fundamentals: A strapdown navigation algorithm [16] processes the vector of acceleration and turn rate measurements $\mathbf{z}_l = [\mathbf{a}_l \ \boldsymbol{\omega}_l]^T$, which is provided by the inertial sensors, to compute position $\mathbf{r}_l$, velocity $\mathbf{v}_l$, and attitude $\boldsymbol{\Psi}_l$. In parallel an extended Kalman filter is used to estimate the errors of the strapdown calculations. Typically 15 states are estimated by the filter [5], [15]: position errors $\delta\mathbf{r}_l$, velocity errors $\delta\mathbf{v}_l$, attitude errors $\delta\boldsymbol{\Psi}_l$, accelerometer biases $\delta\mathbf{a}_l$, and gyroscopic biases $\delta\boldsymbol{\omega}_l$. The error estimates $\delta\mathbf{r}_l$, $\delta\mathbf{v}_l$, and $\delta\boldsymbol{\Psi}_l$ are perturbations around the filter operating point $\mathbf{r}_l$, $\mathbf{v}_l$, $\boldsymbol{\Psi}_l$ that is calculated by the strapdown algorithm.

Recalling III-A the lower filter architecture is provides estimates of position, velocity, attitude, and sensor errors in terms of a Gaussian PDF. In the subsequent processing only position and heading are states of interest and we write for concise notation

$$\mathbf{x}_l = \begin{pmatrix} \mathbf{r}_l \\ \Psi_l \end{pmatrix} \ , \tag{20}$$

whereas Ψ_l is the yaw angle derived from $\boldsymbol{\Psi}_l$. From the posterior PDF of the lower filter the (marginalized) posterior $p(\mathbf{x}_l|\mathbf{Z}_l)$ can be derived straightforward.

2) Rest Phase Detection: The reliable identification of the foot's rest phases is crucial for the update of the lower filter. Different approaches have been proposed to trigger the ZUPT measurement [5], [6]. Here we basically follow these ideas and monitor the magnitude of the acceleration vector [6], which is sensed by the accelerometer triad. If the signal remains within a threshold interval around earth gravity for a certain time interval ZUPTs are triggered until the threshold condition is violated. In our approach the ZUPT detection is also used to trigger the update of the upper filter. Each time a ZUPT is

triggered in the lower filter the elapsed time since the last update of the upper filter is checked. If this time exceeds a certain threshold, a new update of the upper filter is initiated.

3) The Step Sensor: The lower filter is used to process the high rate inertial measurements. To exploit them in the upper filter a (virtual) step sensor is derived from the lower filter in order to provide a measure of the traveled distance and the change in heading for each step the pedestrian makes.

To provide the step measurements the following operations are performed at the interface between the lower filter and the virtual step sensor: Each time a new upper filter cycle (k-cycle) is triggered (III-C.2) the expectation of the lower filter $\hat{\mathbf{x}}_l$ is stored in the variable $\hat{\mathbf{x}}_L \widehat{=} \hat{\mathbf{x}}_l$ with $L = k$. Please note that variables associated to the lower filter are indicated by the subscript $(\bullet)_L$ for those time instances l for which k-cycles are triggered. Introducing the step displacement variable $\Delta\mathbf{x}_L = \mathbf{x}_L - \mathbf{x}_{L-1}$ its expectation is almost independent from previous steps due to the ZUPTs that are applied. Thus we have $\Delta\hat{\mathbf{x}}_L = \mathbb{E}(\Delta\mathbf{x}_L|\mathbf{Z}_L)) \approx \mathbb{E}(\Delta\mathbf{x}_L|\mathbf{Z}_L \backslash \mathbf{Z}_{L-1})$ and may write for the displacement with respect to the coordinate system of the lower filter

$$\begin{aligned} \Delta\hat{\mathbf{x}}_L &= \hat{\mathbf{x}}_L - \hat{\mathbf{x}}_{L-1} && (21)\\ &= \begin{pmatrix} \hat{\mathbf{r}}_L \\ \hat{\Psi}_L \end{pmatrix} - \begin{pmatrix} \hat{\mathbf{r}}_{L-1} \\ \hat{\Psi}_{L-1} \end{pmatrix} && (22)\\ &= \begin{pmatrix} \Delta\hat{\mathbf{r}}_L \\ \Delta\hat{\Psi}_L \end{pmatrix} . && (23) \end{aligned}$$

As final measure the displacement with respect to the heading at the previous k-cycle is computed and we have

$$\mathbf{z}_k = \begin{pmatrix} \mathbf{C}^T(\Psi_\varepsilon)\mathbf{C}^T(\Psi_{L-1})\Delta\hat{\mathbf{r}}_L \\ \Delta\hat{\Psi}_L \end{pmatrix} . \quad (24)$$

The average heading misalignment of the inertial sensor platform with respect to the pedestrian's heading is given by the angle Ψ_ε, which has to be fixed initially.

IV. Extended Model

An obvious extension for the integration of foot-mounted inertial sensors is to take benefit of a pair of platforms, whereas one is mounted on each of the pedestrian's feet respectively. Unlike the conventional integration approach, which is based on a single Kalman filter, the cascaded architecture is flexible with respect to the use of a further foot-mounted platform. To integrate the pair of platforms for each of the two feet a Kalman filter may be used to estimate the stepwise position displacement and heading change respectively, such that the lower part of the cascaded architecture shown in Figure 1 is just doubled. In this case both lower filters provide their step-measurements to the upper particle filter.

Due to the nature of a pedestrian movement the step measurements of the lower filters normally arrive asynchronous. To solve this issue the use of a simple mechanical pedestrian model is proposed now.

A. Pedestrian Model

So far we have assumed that the position of the pedestrian's foot coincides with its body position. If two platforms are used it needs to be addressed with respect to which initial state the displacement estimates are sensed respectively. To ease these considerations we use a simple physical interpretation. As illustrated in Figure 3 the body center may be assumed to be on the center of a line connecting the centers of both feet. It can be derived easily by geometrical considerations that during travel and turn of each of the two feet the body center and heading undergoes a change of exact the half of the feet ones. Thus each of the step-measurements provided by the lower filters actually senses the doubled displacement and heading change with respect to the body center. Hence the extended vector of measurements is

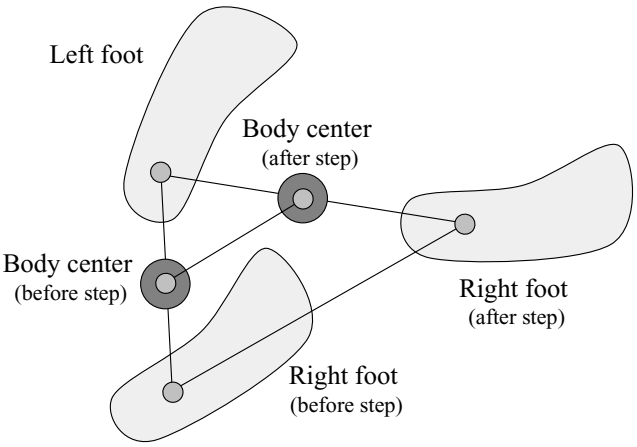

Fig. 3. Mechanical pedestrian model. The body center is assumed to be centered on connecting line of the feet.

$$\mathbf{z}_k = \left[\mathbf{z}_k^r, \mathbf{z}_k^l\right]^T , \quad (25)$$

and we may write for the right foot measurements

$$\mathbf{z}_k^r = 2 \cdot \begin{pmatrix} \Delta\mathbf{r}_k \\ \Delta\Psi_k \end{pmatrix} + \mathbf{n}_\Delta , \quad (26)$$

and correspondingly for the left side

$$\mathbf{z}_k^l = 2 \cdot \begin{pmatrix} \Delta\mathbf{r}_k \\ \Delta\Psi_k \end{pmatrix} + \mathbf{n}_\Delta . \quad (27)$$

B. Error Analysis

As the step measurements are assumed to be superimposed by Gaussian noise according to (11) and (26), (27) respectively, an analysis of the achievable dead-reckoning performance may be carried out analytically. For the analysis we assume a free space scenario, whereas the step-measurement likelihoods are far tighter than the dynamic restrictions that are given by the probabilistic pedestrian movement model. In this case the influence of the movement model becomes negligible, as the the error performance is driven almost solely by the noise of the step-measurements and the pedestrians trajectory.

As the movement model given by (13) and (14) is nonlinear due to the term $\mathbf{C}(\Psi)$, we restrict the analysis with respect to the error magnitude. Given the errors are small, we may linearize the system dynamics for a given state to obtain the linear small-scale error dynamic equations. A truncated Taylor-

series expansion of the full system equations is generally used for the linearization procedure [16]. Following this approach the transition equation for the error state space $\delta\mathbf{x}$ can be shown to be

$$\delta\mathbf{x}_k = \underbrace{\begin{pmatrix} 1 & 0 & 0 & g_1 & c_{11} & c_{12} & 0 & 0 \\ 0 & 1 & 0 & g_2 & c_{21} & c_{22} & 0 & 0 \\ 0 & 0 & 1 & 0 & 0 & 0 & 1 & 0 \\ 0 & 0 & 0 & 1 & 0 & 0 & 0 & 1 \\ 0 & 0 & 0 & 0 & 0 & 0 & 0 & 0 \\ 0 & 0 & 0 & 0 & 0 & 0 & 0 & 0 \\ 0 & 0 & 0 & 0 & 0 & 0 & 0 & 0 \\ 0 & 0 & 0 & 0 & 0 & 0 & 0 & 0 \end{pmatrix}}_{\mathbf{\Phi}_k} \cdot\delta\mathbf{x}_{k-1} \ . \quad (28)$$

The elements $c_{i,j}$ denote the respective element at row i and column j of the matrix $\mathbf{C}(\Psi_{k-1})$. The terms g_1 and g_2 are the respective elements of the vector

$$\mathbf{g} = \mathbf{C}'(\Psi_{k-1})\Delta\mathbf{r}_k \ , \quad (29)$$

whereas the derivative of the rotation matrix is

$$\mathbf{C}'(\Psi) = \frac{\mathrm{d}\mathbf{C}(\Psi)}{\mathrm{d}\Psi} \ . \quad (30)$$

Given the linear error model defined in (28) the system can be analysed using the well known framework of Kalman filtering [19]. Given the initial state $\mathbf{x}_0 = \bar{\mathbf{x}}_0$ and the associated error covariance $\mathbf{P}_0 = \bar{\mathbf{P}}_0$, the incoming step-measurement at time step k affects the covariance through

$$\mathbf{P}_k = (\mathbf{I} - \mathbf{K}_k\mathbf{H})\mathbf{P}_k^- \ , \quad (31)$$

with the Kalman gain

$$\mathbf{K}_k = \mathbf{P}_k^-\mathbf{H}^T(\mathbf{H}\mathbf{P}_k^-\mathbf{H}^T + \mathbf{R})^{-1} \ , \quad (32)$$

the a priori covariance

$$\mathbf{P}_k^- = \mathbf{\Phi}_k\mathbf{P}_{k-1}\mathbf{\Phi}_k^T + \mathbf{Q} \ , \quad (33)$$

and the transition matrix $\mathbf{\Phi}_k$ as defined in (28). For the other matrices we have

$$\mathbf{H} = \begin{bmatrix} \mathbf{0}_{4x4} & \mathbf{I}_{4x4} \end{bmatrix} \ , \quad (34)$$

$$\mathbf{R} = \mathrm{diag}(\begin{bmatrix} \sigma_x^2 & \sigma_y^2 & \sigma_z^2 & \sigma_\Psi^2 \end{bmatrix}) \ , \quad (35)$$

$$\mathbf{Q} = \begin{bmatrix} \mathbf{0}_{4x4} & \mathbf{0}_{4x4} \\ \mathbf{0}_{4x4} & \mathbf{Q}_{4x4}^{ped} \end{bmatrix} \ . \quad (36)$$

Note that $\mathbf{Q}^{ped}$ is matched to pedestrian movement [18]. Since we have $\mathbf{Q}_{i,j}^{ped} >> \mathbf{R}_{i,j}$ for all matrix elements i, j, the influence of $\mathbf{Q}^{ped}$ on the error performance is almost negligible here.

Given a true state trajectory $\mathbf{X}_k \widehat{=} \{\mathbf{x}_q, q = 1, \ldots, k\}$, the corresponding error covariance may now be calculated recursively using (31). For the analysis of the double-platform scenario the same approach is still viable. Nevertheless it has to be taken into account that in this case the step-measurements follow (26) and (27). Thus we have for the extended scenario

$$\mathbf{H} = \begin{bmatrix} \mathbf{0}_{4x4} & 2\cdot\mathbf{I}_{4x4} \end{bmatrix} \ . \quad (37)$$

V. Results

The performance achievements of shoe-mounted INS as stand-alone or coupled with GNSS and / or magnetometer has been widely reported in the literature, for example in [5]. In this paper we present results that consider the incorporation of nonlinear map-matching as well as the extension towards a pair of foot-mounted platforms. Simulation results and experimental results are shown.

A. Simulation

The performance advance with a pair of platforms is assessed by computer simulations. The simulation scenario is the following: Two pedestrians, one of them using a single shoe-mounted platform and the other a pair them, start dead-reckoning from a known initial position and with known initial heading. The step-measurements are assumed to arrive with a rate of 1 Hz respectively, whereas the measurements of the second platform are delayed by 0.5s. An error analysis corresponding to IV-B is carried out along.

The advantage of the double platform approach is shown in Figure 4(a). For the step-measurement noise $\mathbf{n}_\Delta$ we assumed standard deviations of $\sigma_x = \sigma_y = \sigma_z = 0.1$m and $\sigma_\Psi = 2°$. The true state trajectory is static. As the number of available measurements is doubled effectively for the double platform approach, the variance is reduced by a factor of 2 compared to the single platform case. An alternative interpretation of the result is given as follows: As it may be derived from the mechanical pedestrian model, the effective variance of the step-measurement noise with respect to the body movement is decreased by a factor of four compared to the foot movement. Along the use of a second platform doubles the number of required filter recursions due to the additional measurements, leading to a variance increase by a factor of two in turn, such that as final advance a performance gain by a factor of two is reached.

Figure 4(b) shows the result of the corresponding error analysis. As illustrated the simulation results are very close to the behavior that is expected from the error analysis. This implies that the loss due to the suboptimal particle filter implementation is small.

B. Experiment

The chosen experimental scenario is the following: a pedestrian moves through a building, using only the shoe-mounted INS. The initial position is unknown, and no source of absolute position information such as GNSS is used. The only other information available to the upper fusion filter is the building layout (floor-plan). We also assume that the user is within the specified building, and on a certain known floor.

As Fig. 5 shows, the upper fusion filter - a particle filter - starts with a uniform distribution of particles in the known area. Each particle, according to (9), includes its location and current heading. Over time only those particles will survive which are compatible with the layout of the floor-plan. In other words, those hypotheses of the state space will survive, which when moved according to thee lower fusion filter's

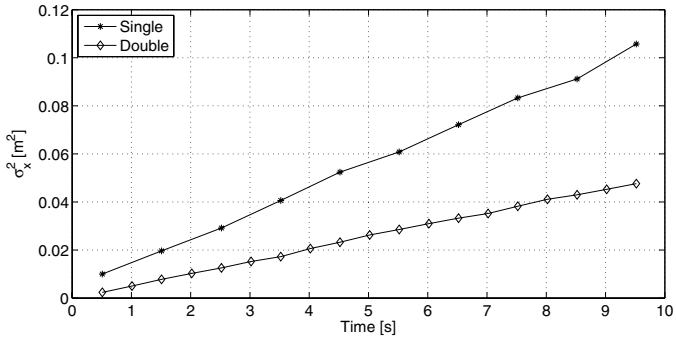

(a) SMC simulation

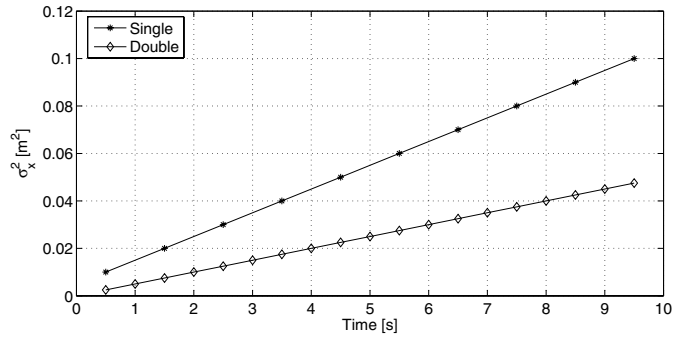

(b) Error analysis

Fig. 4. Performance of single and double platform approach during first 10s of dead-reckoning. The simulation results shown in 4(a) are averaged over 750 Monte-Carlo runs using $N_p = 2000$ particles respectively.

estimate, have not crossed a wall. At first there are many such hypotheses, some moving in different directions compared to the true one, but over the course of time, only one hypothesis (the correct one), survives. In our case this was achieved in roughly one minute of walking.

Naturally, the rate of convergence and the reduction of modes will be a function of the actual route which was walked and of its relation to the floor plan restrictions. In an large hall without walls there will only be moderate reduction on the size of the remaining mode compared to the case with many walls. It should be noted that the surviving modes are "randomly" distributed across the layout and bear no relationship to the correct location (except the true mode, of course). As can be seen from the third time slice (25 s.) the true mode has already achieved its steady-state local uncertainty (of roughly the dimension of the corridor width). This implies that additional position information can be of significant value even if this is quite coarse (e.g. on the order of 10-50 meters).

VI. Conclusions

In this paper a method for integrating shoe-mounted inertial sensors into a Bayesian location estimation framework is presented. The approach is characterized by a cascaded filter architecture, which allows to exploit the synergy between a conventional shoe-mounted INS and a nonlinear pedestrian movement model in an indoor scenario. An advantage of the proposed integration algorithm is that each level of the cascaded architecture can operate at an update rate appropriate to the scale: at 100 Hz or higher for the stride estimation

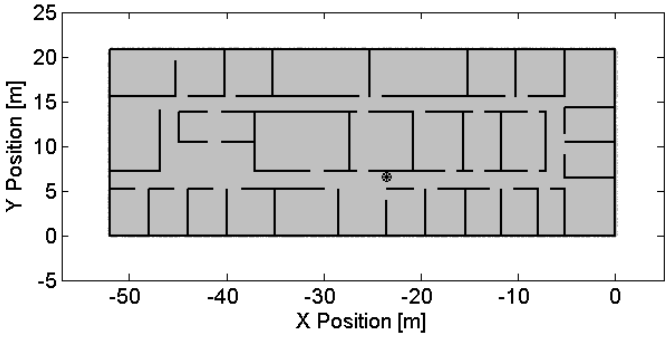

(a) Initial state

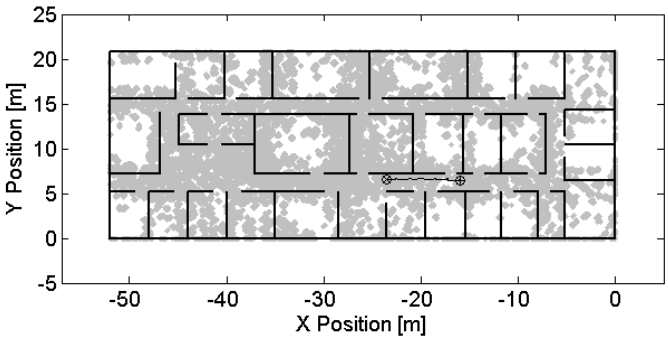

(b) After 10s

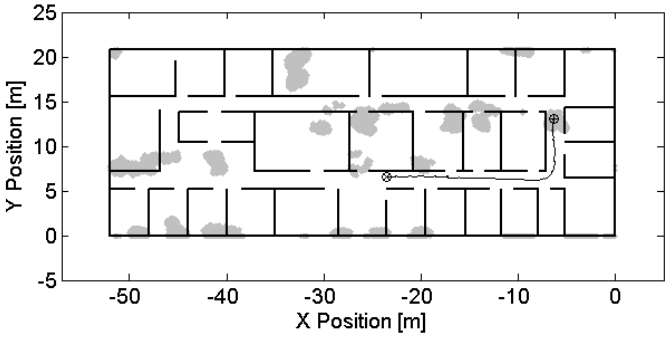

(c) After 25s

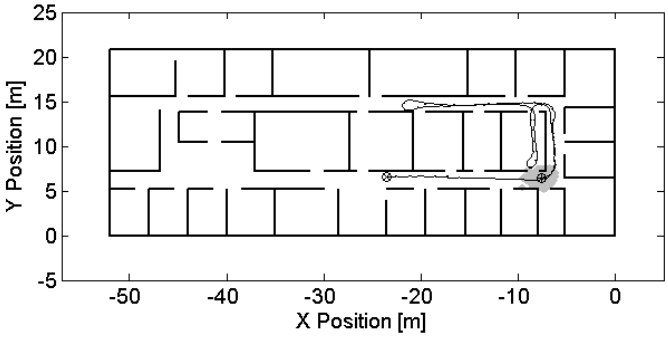

(d) After 80s

Fig. 5. Integration with map-matching in the upper particle filter: A pedestrian wearing the foot-mounted sensor walked the indicated track (black). At each figure the posterior position estimate (gray) becomes increasingly accurate, after 80s it is unimodal.

and roughly at step-rate for the upper fusion layer. It was shown that the use of a pair of platforms improves the dead-reckoning, whereas the variance is reduced by a factor of 2 thanks to the introduced pedestrian model. Based on experimental data it is shown that a moving pedestrian can be localized in a building just by using a foot-mounted 6DOF inertial platform and map matching without using any additional sensors and without the need to determine the pedestrian's initial position or heading in an alignment procedure. Furthermore, the experiment shows that due to the implicit map matching the uncertainty about the pedestrian's location decreases if the movement is suitable, which can lead to long-term stability in an indoor navigation scenario.

REFERENCES

[1] V. Gabaglio and B. Merminod, "Real-time calibration of length of steps with GPS and accelerometers," in *Proceedings of the ENC GNSS 1999*, Genova, Italia, Oct. 1999, pp. 599–605.

[2] Q. Ladetto, "On foot navigation: continuous step calibration using both complementary recursive prediction and adaptive Kalman filtering," in *Proceedings of the 13th International Technical Meeting of the Satellite Division of the Institute of Navigation ION GPS 2000*, 2000.

[3] J. Collin, O. Mezentsev, and G. Lachapelle, "Indoor positioning system using accelerometry and high accuracy heading sensors," in *Proceedings of the 16th International Technical Meeting of the Satellite Division of the Institute of Navigation ION GPS/GNSS 2003*, Portland, Orgeon, USA, Sept. 2003.

[4] D. Kubrak, C. Macabiau, and M. Monnerat, "Performance analysis of MEMS based pedestrian navigation systems," in *Proceedings of the 18th International Technical Meeting of the Satellite Division of the Institute of Navigation ION GNSS 2005*, Long Beach, California, USA, Sept. 2005.

[5] E. Foxlin, "Pedestrian tracking with shoe-mounted inertial sensors," *IEEE Computer Graphics and Applications*, vol. 25, no. 6, pp. 38–46, Nov. 2005.

[6] S. Godha, G. Lachapelle, and M. E. Cannon, "Integrated GPS/INS system for pedestrian navigation in a signal degraded environment," in *Proceedings of the 19th International Technical Meeting of the Satellite Division of the Institute of Navigation ION GNSS 2006*, Fort Worth, Texas, USA, Sept. 2006.

[7] S. Beauregard, "Omnidirectional pedestrian navigation for first responders," in *Proceedings of the 4th Workshop on Positioning, Navigation and Communication, 2007, WPNC07*, Hannover, Germany, Mar. 2007, pp. 33–36.

[8] P. D. Groves, G. W. Pulford, C. A. Littlefield, D. L. J. Nash, and C. J. Mather, "Inertial navigation versus pedestrian dead reckoning: Optimizing the integration," in *Proceedings of the 20th International Technical Meeting of the Satellite Division of the Institute of Navigation ION GNSS 2007*, Fort Worth, Texas, USA, Sept. 2007, pp. 2043—2055.

[9] B. Krach and P. Robertson, "Integration of foot-mounted inertial sensors into a Bayesian location-estimation framework," in *Proceedings of the 5th Workshop on Positioning, Navigation and Communication, 2008, WPNC08*, Hannover, Germany, Mar. 2008.

[10] Widyawan, M. Klepal, and S. Beauregard, "A backtracking particle filter for fusing building plans with PDR displacement estimates," in *Proceedings of the 5th Workshop on Positioning, Navigation and Communication, 2008, WPNC08*, Hannover, Germany, Mar. 2008.

[11] S. Arulampalam, S. Maskell, N. Gordon, and T. Clapp, "A tutorial on particle filters for online nonlinear/non-Gaussian Bayesian tracking," *IEEE Transactions on Signal Processing*, vol. 50, no. 2, pp. 174–188, Feb. 2002.

[12] B. Ristic, S. Arulampalam, and N. Gordon, *Beyond the Kalman Filter - Particle Filters for Tracking Applications*. Boston-London: Artech House, 2004.

[13] A. Doucet, N. de Freitas, and N. Gordon, Eds., *Sequential Monte Carlo Methods in Practice*. New York: Springer, 2001.

[14] M. Angermann, J. Kammann, P. Robertson, A. Steingass, and T. Strang, "Software representation for heterogeneous location data sources using probability density functions," in *International Symposium on Location Based Services for Cellular Users, LOCELLUS 2001*, Munich, Germany, Feb. 2001, pp. 107–118.

[15] M. Grewal, L. Weill, and A. Andrews, *Global Positioning Systems, Inertial Navigation, and Integration*, 2nd ed., ser. IEE Radar, Navigation and Avionics Series. New York: John Wiley & Sons, Inc., 2001, vol. 5.

[16] D. H. Titterton and J. L. Weston, *Strapdown inertial navigation technology*, 2nd ed., ser. IEE Radar, Navigation and Avionics Series. London: Peter Peregrinus Ltd., 2004, vol. 5.

[17] "Advances in navigation sensors and integration technology," NATO RTO Eductional Notes, RTO-EN-SET-064, AC/323(SET-064)TP/43, NATO RTO, Feb. 2004.

[18] M. Khider, S. Kaiser, P. Robertson, and M. Angermann, "A novel movement model for pedestrians suitable for personal navigation," in *Proceedings of the Institute of Navigation National Technical Meeting 2008*, San Diego, California, USA, Jan. 2008.

[19] P. Maybeck, *Stochastic Models, Estimation and Control, Volume I*, ser. Mathematics in Science and Engineering. New York: Academic Press, Inc., 1979, vol. 141.